

# Context-Based Multimodal Fusion

Bilal FAYE<sup>1</sup>, Hanane AZZAG<sup>2</sup>, Mustapha Lebbah<sup>3</sup>, Djamel BOUCHAFFRA<sup>4</sup>  
 e-mail: faye@lipn.univ-paris13.fr, azzag@univ-paris13.fr, mustapha.lebbah@uvsq.fr,  
 djamel.bouchaffra@gmail.com

**Abstract**—The fusion models, which effectively combine information from different sources, are widely used in solving multimodal tasks. However, they have significant limitations related to aligning data distributions across different modalities. This challenge can lead to inconsistencies and difficulties in learning robust representations. Alignment models, while specifically addressing this issue, often require training "from scratch" with large datasets to achieve optimal results, which can be costly in terms of resources and time.

To overcome these limitations, we propose an innovative model called Context-Based Multimodal Fusion (CBMF), which combines both modality fusion and data distribution alignment. In CBFM, each modality is represented by a specific context vector, fused with the embedding of each modality. This enables the use of large pre-trained models that can be frozen, reducing the computational and training data requirements. Additionally, the network learns to differentiate embeddings of different modalities through fusion with context and aligns data distributions using a contrastive approach for self-supervised learning. Thus, CBFM offers an effective and economical solution for solving complex multimodal tasks.

## I. INTRODUCTION

In the contemporary landscape of information abundance, the integration of diverse modalities, such as text, image, and video, holds substantial promise for capturing intricate cross-domain relationships. Multimodal representation learning has emerged as a pivotal field for achieving this integration, offering the potential for a unified understanding of information from various sources [1]–[3]. However, a central challenge lies in multimodal fusion, the process of harmonizing disparate modalities into a cohesive and meaningful representation space, while simultaneously addressing the complexities of aligning and integrating information from multiple modalities. Multimodal fusion involves combining information from different sensory channels, whereas multimodal alignment specifically focuses on ensuring that corresponding elements or features in different modalities are properly synchronized and matched for effective integration and analysis.

In the realm of multimodal fusion, as outlined in [4], four fundamental types are recognized: early fusion, which involves combining raw features from different modalities at the input level before passing them through a shared representation network; late fusion, which integrates the outputs of separate modality-specific networks at a higher level, typically through techniques such as averaging or concatenation; intermediate fusion, which combines information from different modalities at multiple

intermediate stages of processing, enabling more nuanced integration and interaction between modalities; and hybrid fusion, which combines elements of multiple fusion techniques, leveraging their respective strengths to achieve improved performance or flexibility in handling diverse types of data and tasks.

Despite the effectiveness of multimodal fusion approaches, challenges such as information misalignment and modality discrepancy may arise, limiting their overall performance. To address these limitations, multimodal alignment techniques [5]–[7] are introduced, focusing on synchronizing and harmonizing information across modalities for more cohesive and meaningful integration of multimodal data. Furthermore, multimodal alignment techniques, while addressing these challenges, often encounter limitations themselves, notably in computational expense. This is primarily due to the necessity of utilizing large models trained from scratch on extensive datasets to achieve optimal alignment across modalities.

To address these challenges, we present Context-Based Multimodal Fusion (CBMF), an end-to-end method that combines multimodal fusion and alignment. CBFM utilizes a frugal approach that involves aligning large pre-trained models by freezing them during the training process. To achieve optimal results, CBFM trains a single deep fusion small encoder that fuses the context information and model embedding output of each aligned model. This method allows to leverage the benefits of large pre-trained models while aligning them on a small-scale dataset with low computational cost. Our contributions can be summarized as follows:

- **Frugal Approach:** CBFM introduces a frugal approach to multimodal fusion and alignment, which involves aligning large pre-trained models by freezing them during the training process. This approach significantly reduces computational costs while still achieving effective alignment across modalities.
- **Context-Based Fusion:** CBFM incorporates context-based fusion, where a single deep fusion small encoder is trained to fuse both the context information and model embedding output of each aligned model. By considering context, CBFM enhances the coherence and meaningfulness of the multimodal fusion process.

- **Leveraging Pre-Trained Models:** CBMF leverages the benefits of large pre-trained models while aligning them on a small-scale dataset. By utilizing pre-trained models and optimizing alignment with a small-scale dataset, CBMF achieves efficient and effective multimodal fusion and alignment without the need for extensive computational resources.

## II. STATE-OF-ART

In the context of deep learning, multimodal refers to the integration of information from multiple modalities, such as text, images, audio, and video, into a unified representation or model [8, 9]. This approach allows for a more comprehensive understanding of data by leveraging information from different sources. Various methods of multimodal integration, such as fusion and alignment, have been proposed in recent research [1]–[3, 10]–[12].

The fusion of different modalities involves merging specific features to create a highly informative single representation, a process widely employed for its proven efficacy in various predictive tasks. Consequently, numerous researchers have focused on multimodal fusion, particularly in fields such as computer vision and natural language processing.

Orton et al. [4] categorize fusion into four fundamental types: early, late, intermediate, and hybrid fusion.

Early fusion, also known as feature-level fusion, combines raw features from different modalities at the input level [1, 2, 9, 13]. For example, it has been applied in emotion detection tasks [14] and conversation-based emotion detection [13]. However, it may face challenges such as the modality gap and generating high-dimensional features.

Late fusion, also known as decision-level fusion, involves combining the outputs of separate modality-specific models at a higher level, typically through techniques such as averaging, voting, or stacking [1, 2]. This approach has been widely used in various applications such as sentiment analysis, where the predictions from different modality-specific models are combined to make a final decision [15]. Similarly, in action recognition tasks, late fusion is employed to aggregate predictions from multiple modalities such as RGB, depth, and skeleton data [16]. However, late fusion methods may face challenges in handling discrepancies between modalities and may require careful calibration to achieve optimal performance [17].

Intermediate fusion involves combining information from different modalities at multiple intermediate stages of processing, allowing for more nuanced integration and interaction between modalities [1, 2]. This approach has been utilized in various applications, such as action recognition, where intermediate fusion techniques are used to combine features from different modalities, such as RGB, depth, and optical flow, at multiple stages of a deep neural network [18]. Similarly, in affective computing, intermediate fusion is employed to combine

features extracted from different modalities, such as facial expressions, physiological signals, and linguistic cues, to improve the accuracy of emotion recognition systems [19]. On the other hand, hybrid fusion combines elements of multiple fusion techniques, leveraging their respective strengths to achieve improved performance or flexibility in handling diverse types of data and tasks [1, 2]. For example, in medical image analysis, hybrid fusion techniques are used to combine information from different imaging modalities, such as Magnetic Resonance Imaging (MRI) and Positron Emission Tomography (PET) scans, using both early and late fusion methods to improve diagnostic accuracy [20]. Hybrid fusion has also been applied in natural language processing tasks, where it combines features from text and knowledge graphs to enhance information retrieval and question answering systems [21].

However, despite the advantages offered by multimodal fusion techniques, they are often challenged by issues such as the modality gap, high-dimensional feature representations, and difficulties in effectively integrating information from diverse sources. These limitations can hinder the performance and generalization ability of multimodal systems. Fortunately, multimodal alignment methods have emerged as promising solutions to address these challenges by precisely aligning and integrating information from multiple modalities, thereby enhancing the overall effectiveness of multimodal systems.

Multimodal alignment refers to the process of precisely aligning and integrating information from multiple modalities to achieve a cohesive representation space. This can be achieved through approaches such as contrastive learning [22], masked modeling [23], and encoder-decoder modules [24], which enable the learning of joint representations across modalities by leveraging similarities, context prediction, and translation between modalities, respectively.

Contrastive learning involves maximizing agreement between similar samples while minimizing agreement between dissimilar ones [22]. ConVIRT applies multimodal contrastive learning to medical imaging, integrating visual and textual information for tasks like disease diagnosis [25]. CLIP extends this approach to a larger scale, enabling a single model to understand concepts across modalities [26]. ALIGN addresses noisy datasets, ensuring robust performance [27], while GLIP applies CLIP to object detection tasks [28]. These advancements highlight contrastive learning's versatility in diverse fields. Masked modeling, another approach in multimodal learning, involves training models to predict missing parts of input data, effectively learning contextual relationships between different modalities [23]. For example, VisualBERT extends this approach to visual data by masking certain regions in images and predicting them based on textual context, enabling joint understanding of text and images [7]. On the other hand, encoder-decoder modules are widely used in multimodal architectures to capture interactions between

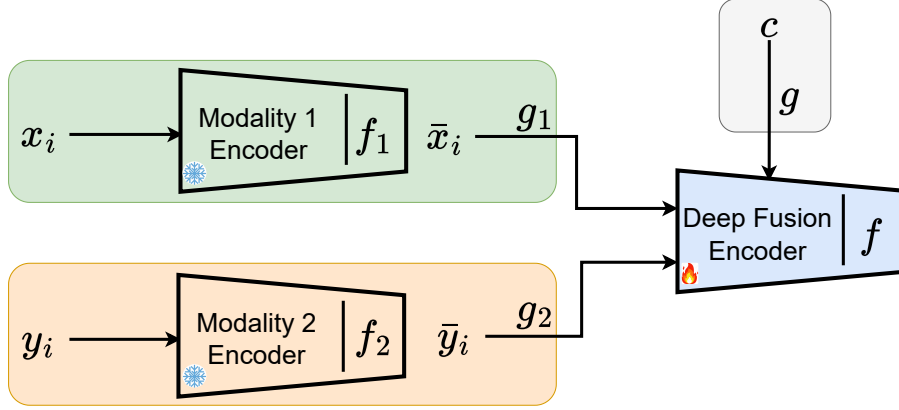


**Fig. 1:** Summary of our CBMF framework. Encoders for individual modalities are pre-trained and kept static, while only the deep fusion encoder undergoes training to ensure cost-effectiveness.

modalities through cross-attention mechanisms [29]. Models like VirTex, PrefixLM, and visualGPT leverage encoder-decoder architectures with cross-attention to achieve state-of-the-art performance in tasks such as image captioning and multimodal translation [30]–[32]. These approaches demonstrate the effectiveness of contrastive learning, masked modeling and encoder-decoder modules in facilitating multimodal understanding across various domains.

Despite their ability to achieve high performance, multimodal alignment techniques often face challenges due to the computational expense associated with training large models from scratch on extensive datasets to achieve optimal alignment across modalities.

### III. OUR PROPOSED METHOD

Context-Based Multimodal Fusion (CBMF) is an approach that integrates multimodal fusion and alignment techniques to effectively align extensive pre-trained models in an efficient manner. To do it, we train only a shared encoder called Deep Fusion Encoder (DFE), that takes as input embeddings of pre-trained models we want to align. Models can have different distribution, to resolve it, we use context vector that allows DFE, to make difference from embeddings of each model, this context vector is specific for each models and is fused to embeddings of correponding model, by the DFE.

Let  $\mathbf{X}$  represent the dataset for modality 1 and  $\mathbf{Y}$  represent the dataset for modality 2. Each pair in the dataset can be denoted as  $(\mathbf{x}_i, \mathbf{y}_i)$ , where  $\mathbf{x}_i$  is an instance from modality 1 and  $\mathbf{y}_i$  is the corresponding instance from modality 2. So, the paired dataset can be represented as:

$$\{(\mathbf{x}_1, \mathbf{y}_1), (\mathbf{x}_2, \mathbf{y}_2), \dots, (\mathbf{x}_N, \mathbf{y}_N)\},$$

where  $N$  is the total number of paired instances in the dataset. Our aim is to train a parameterized function  $f$ , referred to as the Deep Fusion Encoder, to effectively align the pre-trained frozen encoder functions  $f_1$  and  $f_2$ . While  $f_1$  handles data from modality 1 and  $f_2$  handles data

from modality 2. To ensure that the outputs of  $f_1$  and  $f_2$  are projected into the same  $\mathbf{R}^d$  dimension, we incorporate non-linear projections  $g_1$  and  $g_2$ , following the approach outlined in Zhang et al. [25]. Additionally, to enrich the representation, we introduce a context identifier  $\mathbf{c}$  drawn from the set  $\{\mathbf{c}_1 = 1, \mathbf{c}_2 = 2\}$ , which is further enhanced by a function  $g$ .

For each paired input  $(\mathbf{x}_i, \mathbf{y}_i)$ , the CBMF transformation is defined as follows (ref. Figure 2)

$$\begin{aligned} \hat{\mathbf{x}}_i &= f(g_1(f_1(\mathbf{x}_i)) \otimes g(\mathbf{c}_1)), \\ \hat{\mathbf{y}}_i &= f(g_2(f_2(\mathbf{y}_i)) \otimes g(\mathbf{c}_2)) \end{aligned} \quad (1)$$

In this context, the symbol  $\otimes$  represents the fusion operation, which encompasses various fusion techniques including element-wise fusion (such as addition, multiplication, and concatenation) [33] or cross-attention fusion [34] (ref. Figure 1). In the cross-attention method, the context representation serves as the query and can be formulated within  $\mathbf{x}_i$  as follows:

$$\begin{aligned} \mathbf{Q} &= g(\mathbf{c}_1), \\ \mathbf{K} &= \mathbf{V} = g_1(f_1(\mathbf{x}_i)), \\ \text{scores} &= f_s(\mathbf{Q}, \mathbf{K}), \\ \text{Attn} &= \text{SoftMax}(\text{scores}) \cdot \mathbf{V} \end{aligned} \quad (2)$$

where  $f_s$  represents the scoring function [24, 35]–[38].

During training, we extract a minibatch comprising  $M$  input pairs  $(\mathbf{x}_i, \mathbf{y}_i)$  from the  $N$  pairs within the training dataset. Subsequently, we compute their corresponding representation pairs  $(\hat{\mathbf{x}}_i, \hat{\mathbf{y}}_i)$  using Equation 1. The training objective of CBMF encompasses two loss functions. The initial loss function involves a contrastive loss between modality 1 to modality 2 for  $(\hat{\mathbf{x}}_i, \hat{\mathbf{y}}_j)$ :

$$\ell_{ij}^1 = -\log \frac{\exp(\langle \mathbf{x}_i, \mathbf{y}_j \rangle / \tau)}{\sum_{m=1}^M \exp(\langle \hat{\mathbf{x}}_i, \hat{\mathbf{y}}_m \rangle / \tau)} \quad (3)$$

The expression  $\langle \mathbf{x}_i, \mathbf{y}_i \rangle$  denotes the cosine similarity, while  $\tau \in \mathbb{R}^+$  signifies a temperature parameter. This loss function shares the same structure as the InfoNCE loss [39], and minimizing it results in encoders that effectively retain

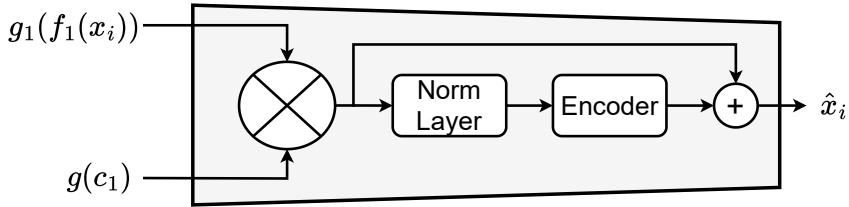


**Fig. 2:** Summary of Deep fusion Encoder (DFE) framework on modality 1.

Dataset	Description	Size
COCO Captions [41]	Description of images in the Microsoft COCO dataset	–
MRPC [42]	Microsoft Research Paraphrase Corpus	–
QQP [43]	Question pairs from the Quora website	–
STS-B [44]	Semantic Textual Similarity Benchmark	–
CIFAR-10 [45]	60,000 32x32 color images in 10 classes	60K images
CIFAR-100 [46]	60,000 32x32 color images in 100 classes	60K images
Tiny ImageNet [47]	Images with dimensions of 64x64 pixels, categorized into 200 classes	110K images
Flickr8k [48]	A collection of 8,000 images with captions	8K images

**TABLE I:** Dataset Descriptions and Sizes

the mutual information between the true pairs through the representation functions [25]. While the modality 1 to modality 2 contrastive loss is asymmetric for each input modality, we consequently introduce a similar contrastive loss from modality 2 to modality 1 as follows:

$$\ell_{ij}^2 = -\log \frac{\exp(\langle \hat{\mathbf{y}}_i, \hat{\mathbf{x}}_j \rangle / \tau)}{\sum_{m=1}^M \exp(\langle \hat{\mathbf{y}}_i, \hat{\mathbf{x}}_m \rangle / \tau)} \quad (4)$$

The matching pairs are situated along the diagonal of the similarity matrix  $(\hat{\mathbf{x}}_i, \hat{\mathbf{y}}_i)$ , which serves as the target for the loss function:

$$t_{ij} = \frac{\exp((\langle \mathbf{x}_i, \mathbf{x}_j \rangle + \langle \mathbf{y}_i, \mathbf{y}_j \rangle) / 2 \cdot \tau)}{\sum_{m=1}^M \exp((\langle \hat{\mathbf{x}}_i, \hat{\mathbf{x}}_m \rangle + \langle \hat{\mathbf{y}}_i, \hat{\mathbf{y}}_m \rangle) / 2 \cdot \tau)} \quad (5)$$

The ultimate training loss is computed by combining the two losses and averaging them over all pairs within each minibatch.

$$\mathcal{L} = \frac{1}{2M} \sum_{i=1}^M \sum_{j=1}^M t_{ij} \cdot \ell_{ij}^1 + t_{ji} \cdot \ell_{ij}^2 \quad (6)$$

In CBMF, leveraging context offers two advantages. Firstly, it enables a single encoder to handle embeddings from various models, which may have different distributions. Incorporating context helps the encoder distinguish between embeddings of each model, enhancing representation. Additionally, by freezing pre-trained models during training, only the DFE is learned, reducing the number of parameters. Secondly, context can serve as an implicit prior, as discussed in Wang et al. [40], facilitating the simultaneous learning of implicit and explicit knowledge for improved representation. Unlike methods that focus solely on aligning specific modalities, CBMF is versatile and can be used efficiently to align any models on a small and large scale dataset, facilitating the transfer of the learned encoder into downstream tasks.

#### IV. EXPERIMENTS

In this section, we present two distinct application methods of Context-Based Multimodal Fusion (CBMF): 1) aligning two different models with the same modality (text), 2) aligning two different modalities (text and image). The models underwent training using the COCO Captions dataset [41], followed by validation across various tasks such as semantic similarity measurement, image classification tasks and image-text retrieval employing datasets listed in Table I.

##### A. Experimental setup

In both experiments, pre-trained models are employed: BERT [49], RoBERTa [50], and Vision Transformer (ViT) [51]. In the CBMF approach, all these models are frozen, and only the Deep Fusion Encoder (DFE) is trained (see Figure 2). To ensure a parsimonious model, a compact architecture is utilized, comprising a fusion layer (employing either element-wise method or cross-attention method), followed by Layer Normalization, then a transformer block with 4 attention heads, succeeded by a residual connection layer to mitigate information loss. The temperature parameter ( $\tau$ ), which regulates the range of logits in the softmax function, is directly optimized during training as a log-parameterized multiplicative scalar to prevent it from becoming a hyper-parameter (see Section III). All models undergo training for 500 epochs with early stopping based on validation loss.

##### B. Enhancing Text-Text Fusion

The goal of this experimentation is to align two pre-trained models, BERT and RoBERTa. These models are commonly used across various contexts to measure text similarity but have limitations in capturing high-level semantic similarity effectively. Utilizing CBMF with these two pre-trained models at low cost offers two advantages: 1) enhancing the ability to capture high-level semantic similarity better than baseline models, and 2) aligning the models in the projection

space, thereby preserving the semantic relationship from the original space to the projection space regardless of the model used, thereby improving interpretability and usability across downstream tasks.

To train the model using the CBMF approach, we curated a new dataset from the captions of the COCO Captions dataset using the Sentence-Transformers [52] model. Two captions (text, text) are deemed semantically similar if their similarity score exceeds a threshold of 0.7. We use additive attention [35] as the scoring function  $f_s$ , outlined in Equation 2:

$$f_s(\mathbf{Q}, \mathbf{K}) = \mathbf{W}_1 \cdot \tanh(\mathbf{W}_2 \cdot \mathbf{Q} + \mathbf{W}_3 \cdot \mathbf{K})$$

Here  $\mathbf{W}_1$ ,  $\mathbf{W}_2$  and  $\mathbf{W}_3$  denote learnable parameters initialized randomly. Referring to Equation 1, we define two contexts:  $\{\mathbf{c}_1 = 1, \mathbf{c}_2 = 2\}$ , where  $\mathbf{c}_1$  corresponds to BERT and  $\mathbf{c}_2$  corresponds to RoBERTa.

To validate the trained CBMF model, we assess its performance by comparing it against pre-trained BERT and RoBERTa models in measuring text similarities across three distinct semantic datasets: Quora Question Pairs (QQP), Microsoft Research Paraphrase Corpus (MRPC), and Semantic Textual Similarity Benchmark (STS-B).

**Validation on QQP Dataset:** This dataset tasks with discerning whether a pair of questions holds semantic equivalence. It serves as an apt benchmark for assessing models aimed at gauging question similarity. The dataset comprises two categories: 0, indicating that the pair of questions (Question 1, Question 2) are not semantically similar, and 1 otherwise.

In Table II, the recall scores highlight a notable trend:

Dissimilar Questions				
model	accuracy	precision	recall	F1-score
BERT	40.82	<b>83.38</b>	7.86	14.37
RoBERTa	36.81	0.0	0.0	0.0
CBMF (Ours)	<b>54.79</b>	72.52	<b>45.80</b>	<b>56.14</b>
Similar Questions				
model	accuracy	precision	recall	F1-score
BERT	40.82	38.11	97.39	54.78
RoBERTa	36.81	36.81	<b>100</b>	53.81
CBMF (Ours)	<b>54.79</b>	<b>43.79</b>	81.00	<b>56.89</b>

**TABLE II:** Performance evaluation comparing baseline models (BERT and RoBERTa) with our fusion-trained model (CBMF) using the Quora Question Pairs (QQP) dataset. "Dissimilar Questions" refers to performance on Category 0, while "Similar Questions" pertains to performance on Category 1.

baseline models (BERT and RoBERTa) struggle particularly in classifying "Dissimilar Questions". This challenge is evident as both models tend to err towards categorizing all questions as similar, resulting in their high performance in the "Similar Questions" category. In contrast, our CBMF method showcases improved performance in discerning "Dissimilar Questions". Not only does CBMF surpass the baseline models, but it also effectively leverages the fusion of BERT and RoBERTa representations, demonstrating an enhanced ability to independently classify dissimilar and

similar questions.

### Microsoft Research Paraphrase Corpus (MRPC):

This dataset serves as a popular benchmark for assessing models in paraphrase identification. It tasks with discerning whether two sentences constitute paraphrases of each other. The dataset consists of two categories: 0, indicating that the pair of sentences (Sentence 1, Sentence 2) are dissimilar, and 1 otherwise. The findings displayed in

Dissimilar Sentences				
model	accuracy	precision	recall	F1-score
BERT	64.21	29.26	9.30	14.11
RoBERTa	68.38	0.0	0.0	0.0
CBMF (Ours)	<b>68.62</b>	<b>50.46</b>	<b>41.86</b>	<b>45.76</b>
Similar Sentences				
model	accuracy	precision	recall	F1-score
BERT	64.21	68.81	89.60	77.39
RoBERTa	68.38	68.38	<b>100</b>	<b>81.22</b>
CBMF (Ours)	<b>68.62</b>	<b>75.08</b>	81.00	77.93

**TABLE III:** Performance evaluation comparing baseline models (BERT and RoBERTa) with our fusion-trained model (CBMF) using the Microsoft Research Paraphrase Corpus (MRPC) dataset. "Dissimilar Sentences" refers to performance on Category 0, while "Similar Sentences" pertains to performance on Category 1.

Table III corroborate the insights gleaned from the QQP dataset experiment. Notably, the baseline models BERT and RoBERTa face challenges in accurately grasping semantic connections between sentences, resulting in notably poor performance within the "Dissimilar Sentences" category. In contrast, our CBMF model demonstrates enhanced capability in capturing these relationships across both similar and dissimilar sentence pairs.

**Semantic Textual Similarity Benchmark (STS-B):** STS-B is pivotal for evaluating models in semantic textual similarity. It uses scores from 0 to 5 to denote specific levels of similarity between text pairs. Scores 0 to 1 signify complete dissimilarity, 1 to 2 indicate dissimilarity, 2 to 3 suggest moderate similarity, 3 to 4 denote similarity, and 4 to 5 characterize high similarity or identity. This granularity aids nuanced evaluation of models. For performance evaluation, we employ an error tolerance ( $e$ ) strategy: if the difference between true and predicted similarity falls below  $e$ , it's a positive prediction; otherwise, it's negative. We analyze over 100 error tolerance values from 0.1 to 1. Figure 3 reaffirms and strengthens the findings observed in the QQP and MRPC datasets. Baseline models BERT and RoBERTa demonstrate proficiency in capturing sentences with high semantic similarity, yet exhibit limitations in detecting semantic nuances across diverse similarity levels. Our CBMF method addresses these limitations by enhancing semantic representation, preserving the intricate semantics of the input space through a carefully crafted projection space.

To underscore the versatility of CBMF, the subsequent section will explore its application in fusing two models specialized for representing different modalities.

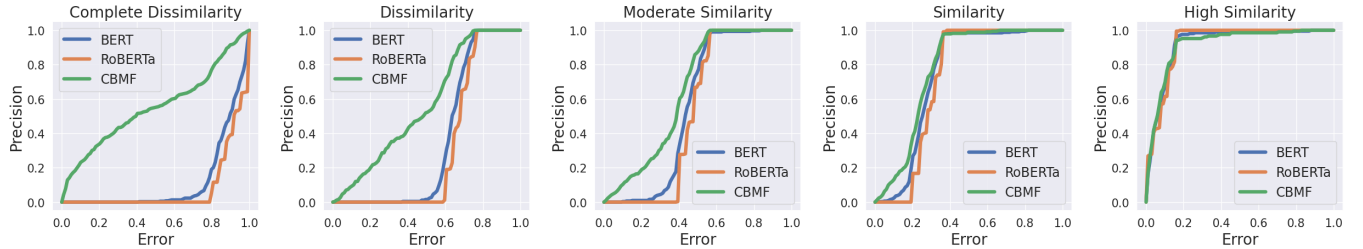


**Fig. 3:** Tracking the evolution of accuracy among baseline models (BERT and RoBERTa) and our CBMF method across various similarity classes, evaluated using the tolerance error method with a comprehensive range of 100 values spanning from 0.1 to 1. This analysis is conducted on the Semantic Textual Similarity Benchmark (STS-B), offering insights into the models' performance across a spectrum of semantic similarity levels.

### C. Enhancing Text-Image Fusion

This experimentation draws inspiration from methods that employ contrastive learning to acquire high-quality visual representations. Similar to conVIRT, which applies this approach in the medical domain, or CLIP, which extends it to large-scale applications, these methods have limitations due to domain specificity or resource-intensive requirements for optimal performance. In this section, we aim to demonstrate, through a cost-effective approach, that our CBMF method can address this issue while achieving excellent performance.

We will utilize pre-trained Vision Transformer (ViT) and BERT models to encode images and captions, respectively. As a baseline, we will employ the conVIRT method, which involves training all pre-trained ViT and BERT models. In contrast, our approach, CBMF, freezes the pre-trained ViT and BERT models and only trains the Deep Fusion Encoder (DFE). In the CBMF method, as described in Equation 1, we adopt two contexts:  $\{c_1 = 1, c_2 = 2\}$ , where  $c_1$  corresponds to BERT, and  $c_2$  corresponds to ViT. We employ two fusion operations: addition and scaled dot-product attention [24]. For the addition operation, following Equation 1, on the first modality, we have:

$$g_1(f_1(\mathbf{x}_i)) + g(c_1)$$

Regarding scaled dot-product attention, as per Equation 2, we have:

$$f_s(\mathbf{Q}, \mathbf{K}) = \frac{\mathbf{Q} \cdot \mathbf{K}^T}{\sqrt{d_k}}$$

where  $d_k$  represents the dimension of the key  $\mathbf{K}$ . All models are trained using identical hyperparameters on the COCO Captions dataset.

Following the training of our models, we proceed to evaluate our pre-trained models on two imaging tasks: image classification tasks and text-image retrieval.

**1) Image Classification Tasks: Zero-shot image classification** involves leveraging existing capabilities to classify images without prior training on specific classes. In this approach, we utilize the names of all classes within the CIFAR-10 dataset as potential text pairings. The goal is to predict the most probable (image, text) pair using CBMF. To elaborate, we first compute the feature embedding of the image ( $f(g_2(f_2(\mathbf{y}_i)) \otimes g(c_2))$ ) and the feature embedding

of the set of possible texts ( $f(g_1(f_1(\mathbf{y}_i)) \otimes g(c_1))$ ) using their respective encoders. Subsequently, we compute the cosine similarity of these embeddings and normalize them into a probability distribution using softmax. Table IV

Model	Accuracy				
	top-1	top-2	top-3	top-4	top-5
conVIRT	62.12	76.53	84.26	89.22	92.95
CBMF-add (Ours)	<b>78.26</b>	<b>88.69</b>	92.5	94.87	96.48
CBMF-dot (Ours)	75.62	87.37	<b>92.62</b>	<b>95.26</b>	<b>97.00</b>

**TABLE IV:** Assessment of zero-shot classification performance on the CIFAR-10 dataset. CBMF-add denotes the CBMF model employing addition for fusion operation, while CBMF-dot represents the CBMF model utilizing scaled dot-product attention for fusion operation.

demonstrates the strong performance of models utilizing the CBMF method (CBMF-add and CBMF-dot) on the CIFAR-10 dataset without retraining. These models, initially trained on the COCO Captions dataset and then adapted to CIFAR-10, which includes two categories absent in the COCO Captions dataset, yield results that surpass the model using the conVIRT approach, which is more resource-intensive.

**Linear Classification:** In this task, we exclusively employ the pre-trained CBMF encoder for images ( $f(g_1(f_1(\mathbf{y}_i)) \otimes g(c_1))$ ) with a linear classifier on the CIFAR-100 dataset. All pre-trained CBMF encoders are kept frozen, and only the linear classifier is trained for 100 epochs. This method enables the evaluation of the extracted image features' quality with the pre-trained CBMF. Models are validated on the test set every 20 epochs during training. Table V presents the strong performance of models

Model	Epoch				
	20	40	60	80	100
conVIRT	55.67	59.22	61.09	62.14	62.71
CBMF-add (Ours)	<b>64.63</b>	<b>66.78</b>	<b>67.93</b>	<b>68.88</b>	<b>69.37</b>
CBMF-dot (Ours)	62.75	63.37	64.57	64.98	65.29

**TABLE V:** Accuracy evaluation of linear classification performance on the CIFAR-100 dataset. CBMF-add refers to the CBMF model utilizing addition for fusion operation, whereas CBMF-dot indicates the CBMF model employing scaled dot-product attention for fusion operation.

utilizing the CBMF method (CBMF-add and CBMF-dot)

for linear classification, consistent with the results observed in zero-shot classification. By leveraging pretrained CBMF models without employing image augmentation and freezing them, our models significantly outperform the approach using conVIRT. This indicates that our method facilitates better quality image features, thereby enhancing the discriminatory ability across categories and consequently improving the classification task.

**Fine-tuning:** In this technique, we adopt a similar approach to linear classification, but unlike in linear classification, the pretrained CBMF models are not frozen. Fine-tuning closely mimics how the pretrained CBMF weights (DFE) are utilized in real-world scenarios. We assess this method on the Tiny ImageNet dataset and train models for 100 epochs without employing any data augmentation. Models are validated on the test set every 20 epochs during training. Table VI corroborates the findings observed in the

Model	Epoch				
	20	40	60	80	100
conVIRT	59.00	62.71	64.45	65.37	65.89
CBMF-add (Ours)	<b>64.49</b>	<b>66.31</b>	<b>67.60</b>	<b>68.12</b>	<b>68.91</b>
CBMF-dot (Ours)	64.21	66.09	66.70	67.74	68.18

**TABLE VI:** Accuracy evaluation of fine-tuning performance on the Tiny ImageNet dataset. CBMF-add refers to the CBMF model utilizing addition for fusion operation, whereas CBMF-dot indicates the CBMF model employing scaled dot-product attention for fusion operation.

zero-shot classification and linear classification experiments. Pre-trained models utilizing the CBMF method can serve as a robust backbone in various tasks, facilitating superior feature representation. CBMF’s frugality obviates the need for extensive datasets and prolonged training times. By combining fusion and alignment, it enables the generation of enhanced models applicable across a wide range of contexts, as demonstrated in the three illustrations.

2) *Image-Text Retrieval:* Image-text retrieval is a task focused on retrieving relevant textual descriptions based on image queries or retrieving relevant images based on textual queries. In essence, it involves searching for images that are semantically related to a given text query or finding textual descriptions that match the content of a given image. In this scenario, we’re working with the Flickr8k dataset, which contains pairs of data consisting of images and corresponding captions. Each image is associated with five captions. Each image  $y_i$  is encoded using pre-trained CBMF  $f(g_2(f_2(y_i)) \otimes g(c_2))$ . Similarly, each caption  $x_i$  undergoes encoding using  $f(g_1(f_1(x_i)) \otimes g(c_1))$ . The goal is to perform image-text retrieval, where images act as queries. We sample captions based on cosine similarity with image features. If a corresponding caption is among the top $_k$  samples for a given image feature, we consider the retrieval successful; otherwise, it’s deemed unsuccessful. We experiment with different values of  $k$ , ranging from 100 to 10,000, to assess retrieval performance across varying levels of relevance. The figure 4 illustrates improved precision

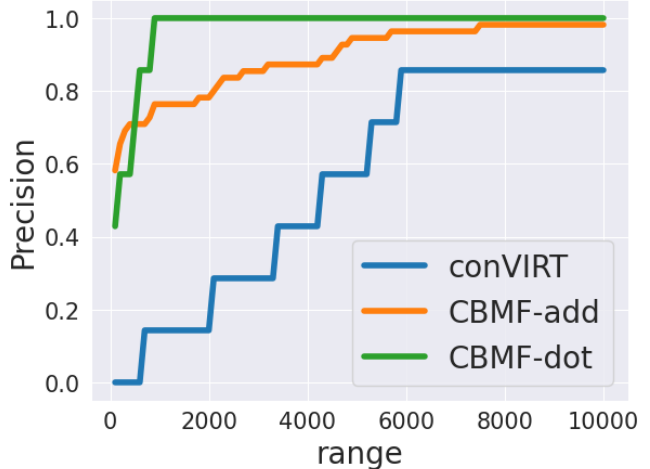


**Fig. 4:** Precision Curve for Image-Text Retrieval on the Flickr8k Dataset. The ‘range’ denotes the top- $k$  values, ranging from 100 to 10,000, where  $k$  represents the number of retrieved results. A retrieval is deemed correct if the true caption is included within the top- $k$  results for each image.

with models employing the CBMF method (CBMF-add and CBMF-dot). A quicker convergence is observed as the tolerance margin increases, with CBMF-dot achieving a precision of 1.0 rapidly. These findings corroborate those of previous experiments with CBMF, which effectively combine thriftiness and performance.

## V. CONCLUSION

In summary, we have introduced a novel method called Context-Based Multimodal Fusion (CBMF), which integrates fusion and contrastive learning for a resource-efficient learning approach. CBMF preserves the semantic information from the original space to the projection space by leveraging large pre-trained models, which remain frozen during the training process. The Deep Fusion Encoder (DFE), the sole neural network trained within the CBMF framework, facilitates the fusion of embeddings from pre-trained models using a learnable parameter referred to as the context, thereby accommodating the distributional shifts across pre-trained models. CBMF exhibits versatility and can be applied across various contexts to align large pre-trained models, consequently yielding enhanced representations for downstream tasks.

## REFERENCES

- [1] T. Baltrušaitis, C. Ahuja, and L.-P. Morency, “A review of multimodal fusion for video understanding,” *International Journal of Computer Vision*, vol. 128, pp. 1039–1052, 2020.
- [2] T. Chen, Y. Xu, T. Luo, C. Li, Y. Xu, and D. Tao, “Multimodal sentiment analysis with word-level fusion and reinforcement learning,” in *Proceedings of the 32nd AAAI Conference on Artificial Intelligence (AAAI)*, pp. 6094–6101, 2018.
- [3] N. Srivastava and R. R. Salakhutdinov, “Multimodal learning with deep boltzmann machines,” in *Advances in neural information processing systems*, pp. 2222–2230, 2012.
- [4] I. J. Orton, “Vision based body gesture meta features for affective computing,” *arXiv preprint arXiv:2003.00809*, 2020.

[5] A. Radford, J. W. Kim, C. Hallacy, A. Ramesh, G. Goh, S. Agarwal, G. Sastry, A. Askell, P. Mishkin, T. Drechsler, *et al.*, “Learning transferable visual models from natural language supervision,” *arXiv preprint arXiv:2103.00020*, 2021.

[6] X. L. Li and P. Liang, “Prefix-tuning: Optimizing continuous prompts for generation,” *arXiv preprint arXiv:2101.00190*, 2021.

[7] L. H. Li, M. Yatskar, D. Yin, C.-J. Hsieh, and K.-W. Chang, “Visualbert: A simple and performant baseline for vision and language,” *arXiv preprint arXiv:1908.03557*, 2019.

[8] J. Ngiam, A. Khosla, M. Kim, J. Nam, H. Lee, and A. Y. Ng, “Multimodal deep learning,” in *Proceedings of the 28th international conference on machine learning (ICML-11)*, pp. 689–696, 2011.

[9] N. Srivastava and R. R. Salakhutdinov, “Multimodal learning with deep boltzmann machines,” in *Advances in neural information processing systems*, pp. 2222–2230, 2012.

[10] P. Gao, W. Zhang, J. Zhang, Y. Li, R. Zhang, and Y. Sun, “A review of multimodal fusion for visual question answering and visual grounding,” *IEEE Transactions on Pattern Analysis and Machine Intelligence*, 2021.

[11] D. Kiela, L. Bottou, and Y. Bengio, “Learning cross-lingual word embeddings with neural language models,” in *Proceedings of the 2014 Conference on Empirical Methods in Natural Language Processing (EMNLP)*, pp. 1001–1011, 2014.

[12] Y. Zhang, Z. Zhang, R. Ji, X. Gao, and Q. Tian, “Recent advances in multimodal fusion for video understanding,” *IEEE Transactions on Pattern Analysis and Machine Intelligence*, 2020.

[13] D. Hazarika, S. Poria, A. Z. Zadeh, E. Cambria, R. Zimmermann, and L.-P. Morency, “Convolutional neural network for text-based emotion recognition in conversations,” in *Proceedings of the 2018 Conference on Empirical Methods in Natural Language Processing*, pp. 3688–3697, 2018.

[14] D. Hazarika, S. Poria, R. Mihalcea, E. Cambria, and R. Zimmermann, “Icon: Interactive conversational memory network for multimodal emotion detection,” in *Proceedings of the 2018 conference on empirical methods in natural language processing*, pp. 2594–2604, 2018.

[15] S. Poria, E. Cambria, D. Hazarika, N. Majumder, and A. Zadeh, “A review of multimodal sentiment analysis,” *Journal of Intelligent Systems*, vol. 26, no. 1, pp. 3–27, 2017.

[16] J. Liu, A. Shahroudy, D. Xu, G. Wang, and L. Yu, “Skeleton-based action recognition with convolutional neural networks,” in *Proceedings of the 2017 IEEE Conference on Computer Vision and Pattern Recognition (CVPR)*, pp. 7370–7378, IEEE, 2017.

[17] Z. Zhang, M. Xu, P. Liu, X. Liu, Y. Wang, Q. Yang, and H. Ji, “Multimodal fusion for emotion recognition from text and speech,” *Proceedings of the 2018 Conference on Empirical Methods in Natural Language Processing (EMNLP)*, pp. 1401–1409, 2018.

[18] J. Zhang, Y. Li, Z. Wu, Y. Liu, and Y. Wang, “Multimodal deep learning for robust rgb-d object recognition,” in *Proceedings of the 2017 IEEE Conference on Computer Vision and Pattern Recognition (CVPR)*, pp. 1346–1354, IEEE, 2017.

[19] J. Liu, Y. Zhang, H. Ji, and H. Chen, “Multimodal fusion for emotion recognition from text and speech,” in *Proceedings of the 58th Annual Meeting of the Association for Computational Linguistics (ACL)*, pp. 2157–2168, 2020.

[20] X. Liu, S. Wang, J. Wang, and K. Li, “Hybrid deep learning for music genre classification,” in *Proceedings of the 28th ACM International Conference on Information and Knowledge Management (CIKM)*, pp. 1231–1240, ACM, 2019.

[21] S. Wang, Y. Zhang, J. Liu, W. Wu, and H.-T. Zheng, “Hybrid hierarchical attention network for text classification,” in *Proceedings of the 43rd International ACM SIGIR Conference on Research and Development in Information Retrieval (SIGIR)*, pp. 735–744, ACM, 2020.

[22] T. Chen, S. Kornblith, M. Norouzi, and G. Hinton, “A simple framework for contrastive learning of visual representations,” *Proceedings of the 37th International Conference on Machine Learning (ICML)*, pp. 1597–1607, 2020.

[23] J. Devlin, M.-W. Chang, K. Lee, and K. Toutanova, “Bert: Pre-training of deep bidirectional transformers for language understanding,” *Proceedings of the 2019 Conference of the North American Chapter of the Association for Computational Linguistics: Human Language Technologies (NAACL-HLT)*, pp. 4171–4186, 2019.

[24] A. Vaswani, N. Shazeer, N. Parmar, J. Uszkoreit, L. Jones, A. N. Gomez, Å. Kaiser, and I. Polosukhin, “Attention is all you need,” in *Advances in neural information processing systems*, pp. 5998–6008, 2017.

[25] L. Zhang, M. Á. Carreira-Perpiñán, and A. Lavie, “Convirt: Contrastive visual representation learning for medical imaging,” *IEEE Transactions on Medical Imaging*, vol. 41, no. 2, pp. 519–531, 2022.

[26] A. Radford, J. W. Kim, C. Hallacy, A. Ramesh, G. Goh, S. Agarwal, G. Sastry, A. Askell, P. Mishkin, J. Clark, *et al.*, “Learning transferable visual models from natural language supervision,” *arXiv preprint arXiv:2103.00020*, 2021.

[27] J. Chung, B. Zoph, A. Srinivas, L. Zhang, W. Yang, B. Zhang, A. Howard, M. Á. Carreira-Perpiñán, and E. D. Cubuk, “Align: Activating latent innovations for multimodal contrastive learning,” in *Advances in Neural Information Processing Systems*, vol. 34, 2021.

[28] W. Liu, L. Zhang, and M. Á. Carreira-Perpiñán, “Glip: Generic latent innovations propagation for multimodal contrastive learning,” in *International Conference on Learning Representations*, 2022.

[29] J. Lu, D. Batra, D. Parikh, and S. Lee, “Vilbert: Pretraining task-agnostic visiolinguistic representations for vision-and-language tasks,” in *Advances in Neural Information Processing Systems*, vol. 33, 2020.

[30] J. Lu, V. Goswami, D. Parikh, and S. Lee, “Virtex: Learning visual representations from textual annotations,” in *European Conference on Computer Vision*, pp. 183–199, Springer, 2020.

[31] X. Li, J. Cheng, J. Yang, R. Yan, P. Xu, F. Dong, X. Sun, and J. Gao, “Prefix-tuning: Optimizing continuous prompts for generation,” in *Advances in Neural Information Processing Systems*, vol. 34, 2021.

[32] C. Li, X. Wei, Y. Zhai, J. Li, J. Gao, and J. Chen, “Visualgpt: Data-efficient image generation using guided variational autoencoders,” in *Proceedings of the AAAI Conference on Artificial Intelligence*, vol. 35, pp. 9707–9715, 2021.

[33] J. Smith and et al., “Multimodal fusion techniques for image and text data,” in *Proceedings of the IEEE Conference on Computer Vision and Pattern Recognition (CVPR)*, 2020.

[34] A. Johnson and et al., “Cross-modal attention mechanisms for multimodal embedding,” in *Advances in Neural Information Processing Systems (NeurIPS)*, 2019.

[35] D. Bahdanau, K. Cho, and Y. Bengio, “Neural machine translation by jointly learning to align and translate,” in *Proceedings of the 3rd International Conference on Learning Representations (ICLR)*, 2015.

[36] M.-T. Luong, H. Pham, and C. D. Manning, “Effective approaches to attention-based neural machine translation,” in *Proceedings of the 2015 Conference on Empirical Methods in Natural Language Processing*, pp. 1412–1421, 2015.

[37] K. Xu and et al., “Show, attend and tell: Neural image caption generation with visual attention,” in *Proceedings of the International Conference on Machine Learning (ICML)*, 2015.

[38] Z. Yang and et al., “Hierarchical attention networks for document classification,” in *Proceedings of the Conference of the North American Chapter of the Association for Computational Linguistics: Human Language Technologies (NAACL-HLT)*, 2016.

[39] A. van den Oord and et al., “Representation learning with contrastive predictive coding,” *arXiv preprint arXiv:1807.03748*, 2018.

[40] C.-Y. Wang, I.-H. Yeh, and H.-Y. M. Liao, “You only learn one representation: Unified network for multiple tasks,” *arXiv preprint arXiv:2105.04206*, 2021.

[41] T.-Y. Lin, M. Maire, S. Belongie, J. Hays, P. Perona, D. Ramanan, P. Dollár, and C. L. Zitnick, “Microsoft coco: Common objects in context,” *Lecture Notes in Computer Science*, vol. 8693, pp. 740–755, 2014.

[42] W. B. Dolan and C. Brockett, “Automatically constructing a corpus of sentential paraphrases,” in *Proceedings of the Third International Workshop on Paraphrasing (IWP2005)*, Association for Computational Linguistics, 2005.

[43] W. Chen, “Quora question pairs,” in *Quora Dataset*, 2018.

[44] D. Cer, M. Diab, E. Agirre, I. Lopez-Gazpio, and L. Specia, “Semeval-2017 task 1: Semantic textual similarity—multilingual and crosslingual focused evaluation,” *arXiv preprint arXiv:1708.00055*, 2017.

[45] A. Krizhevsky and G. Hinton, “Cifar-10 (canadian institute for advanced research),” tech. rep., Technical Report, 2009.

[46] A. Krizhevsky and G. Hinton, “Cifar-100 (canadian institute for advanced research),” tech. rep., Technical Report, 2009.

[47] F.-F. Li, A. Karpathy, and J. Johnson, “Cs231n convolutional neural networks for visual recognition.” <http://cs231n.stanford.edu/>, 2018.

- [48] “Flickr8k.” <http://hockenmaier.cs.illinois.edu/8k-pictures.html>.
- [49] J. Devlin, M.-W. Chang, K. Lee, and K. Toutanova, “Bert: Pre-training of deep bidirectional transformers for language understanding,” *arXiv preprint arXiv:1810.04805*, 2018.
- [50] Y. Liu, M. Ott, N. Goyal, J. Du, M. Joshi, D. Chen, O. Levy, M. Lewis, L. Zettlemoyer, and V. Stoyanov, “Roberta: A robustly optimized bert approach,” *arXiv preprint arXiv:1907.11692*, 2019.
- [51] A. Dosovitskiy, L. Beyer, A. Kolesnikov, D. Weissenborn, X. Zhai, T. Unterthiner, B. Steiner, M. Hein, H. Touvron, A. Hervieu, *et al.*, “An image is worth 16x16 words: Transformers for image recognition at scale,” *arXiv preprint arXiv:2010.11929*, 2020.
- [52] N. Reimers and I. Gurevych, “Sentence-bert: Sentence embeddings using siamese bert-networks,” *arXiv preprint arXiv:1908.10084*, 2019.